

Dynamical scaling, domain-growth kinetics, and domain-wall shapes of quenched two-dimensional anisotropic XY models

Ole G. Mouritsen

Department of Structural Properties of Materials, The Technical University of Denmark, Building 307, DK-2800 Lyngby, Denmark

Eigil Præstgaard

Department of Chemistry, Roskilde University, DK-4000 Roskilde, Denmark

(Received 16 November 1987)

The domain-growth kinetics in two different anisotropic two-dimensional XY-spin models is studied by computer simulation. The models have uniaxial and cubic anisotropy which leads to ground-state orderings which are twofold and fourfold degenerate, respectively. The models are quenched from infinite to zero temperature as well as to nonzero temperatures below the ordering transition. The continuous nature of the spin variables causes the domain walls to be "soft" and characterized by a finite thickness. The steady-state thickness of the walls can be varied by a model parameter, P . At zero temperature, the domain-growth kinetics is found to be independent of the value of this parameter over several decades of its range. This suggests that a universal principle is operative. The domain-wall shape is analyzed and shown to be well represented by a hyperbolic tangent function. The growth process obeys dynamical scaling and the shape of the dynamical scaling function pertaining to the structure factor is found to depend on P . Specifically, this function is described by a Porod-law behavior, $q^{-\omega}$, where ω increases with the wall softness. The kinetic exponent, which describes how the linear domain size varies with time, $R(t) \sim t^n$, is for both models at zero temperature determined to be $n \simeq 0.25$, independent of P . At finite temperatures, the growth kinetics is found to cross over to the Lifshitz-Allen-Cahn law characterized by $n \simeq 0.50$. The results support the idea of two separate zero-temperature universality classes for soft-wall and hard-wall kinetics, and furthermore suggest that these classes become identical at finite temperatures.

I. INTRODUCTION

The domain-growth kinetics in systems undergoing ordering processes after thermal quenching is believed to be governed by a few relevant properties of the systems, whereas most other properties and material-dependent details are irrelevant.¹ Among the most likely candidates for relevant properties are the ordering degeneracy p and the nature of the conservation laws in effect.² Recently, it has also been suggested that domain-wall softness is a relevant property which in some cases may even overrule the relevance of the ground-state degeneracy.³⁻⁶

The present status of the field of domain-growth kinetics is, however, rather unclear. The reasons for this are manifold: (i) Experimental studies are severely hampered by insufficient time resolution and uncontrolled effects due to sample impurities and inhomogeneities. (ii) It is extremely difficult to construct a quantitatively reliable far-from-equilibrium theory,^{1,7-15} in particular for multi-fold degeneracy,^{16,17} which takes local features of the growth mechanism into account. (iii) Computer simulation studies are made difficult by unusual demands to the statistics and, maybe more important, the numerical results are difficult to analyze due to the lack of appropriate theoretical predictions. This is particularly true with regard to temperature and early-time-regime corrections to the asymptotic growth laws and the scaling functions.

Most of the present knowledge of domain-growth kinetics stems from computer simulation studies of two-

dimensional Potts^{4,18-21} and Ising^{2,9,22-36} models with commensurate and incommensurate modulated structures of a variety of symmetries. From these studies it now seems rather well established that the growth processes obey dynamical scaling and that the scaling functions, at least at late times, are rather insensitive to the ordering degeneracy p . The corresponding asymptotic growth law

$$l(t) \sim t^n, \quad (1)$$

which describes how the average linear extension of the domains varies with time t , is found to hold with exponent values $n \simeq \frac{1}{2}$ and $n \simeq \frac{1}{3}$ for nonconserved and conserved order parameter, respectively.³⁷⁻⁴⁰ In the nonconserved case, which we shall restrict ourselves to considering in what follows, the classical Lifshitz-Allen-Cahn^{7,8,41} value $n = \frac{1}{2}$ seems to apply, independent of the value of p , at least for low values of p . For larger values of p , systematic studies¹⁸ of isotropic Q -state Potts models ($p = Q$) as a function of Q have provided some evidence in favor of a Q dependence of n , with n monotonically decreasing to a constant value of $n \simeq 0.41$ for $Q \geq 30$. However, this result has been subject to some controversy and it was suggested²¹ that the Q dependence of the exponent is only apparent and that one, in the asymptotic growth regime, recovers $n \simeq \frac{1}{2}$ for all values of Q . Such a crossover has indeed been found in recent very extensive calculations on ($Q = 48$)-state Potts model arrayed on 1000×1000 lattices.¹⁹ Thus it seems now established that

the domain-growth kinetics for Ising and Potts models with nonconserved order parameter falls into the same universality class, independent of p and independent of the conservation laws for other quantities.³⁶ This class is characterized by the classical Lifshitz-Allen-Cahn growth exponent value $n = \frac{1}{2}$.

A number of computer simulation studies of the domain-growth kinetics in a different class of microscopic lattice models^{3,5,6,42,43} with nonconserved order parameter have, with a few exceptions which will be discussed below,^{33,44} identified a second and separate universality class characterized by $n \simeq \frac{1}{4}$. The models in this class are distinguished from the Ising and Potts models in that they are formulated in terms of continuous single-site variables, such as rotors or XY spins. In contrast to the sharp- (“hard-”) domain walls produced by the discrete variables in Potts and Ising models, the models with the continuous variables support formation of wide- (“soft-”) domain walls during the growth process. Certain anisotropic high- Q Potts models with wide-domain boundaries have also been found to belong to the soft-wall universality class.⁴

From a theoretical point of view it is surprising and somewhat unexpected that softness of domain walls could influence the asymptotic behavior of domain growth. In fact, field-theoretical descriptions of domain growth,²² e.g., ϕ^4 theory, which is formulated in terms of continuous order parameter fields, incorporate smooth walls with the shape of a hyperbolic function. These theories lead to $n = \frac{1}{2}$ for $p = 2$. However, they have a serious shortcoming in that they do not take local features of the growth mechanism into account. On the other hand, Milchev *et al.*³³ recently studied by direct computer simulation a microscopic square-lattice version of the $p = 2$ ϕ^4 model which does incorporate local features of the domain-wall network. They found that their data for nonzero quench temperatures complied with the classical exponent value $n = \frac{1}{2}$ and argued that a separate universality class of soft-wall kinetics may not exist and furthermore inferred that previously studied models yielding $n \simeq \frac{1}{4}$ might cross over to $n \simeq \frac{1}{2}$ at very late times. In addition, Milchev *et al.*³³ presented evidence for the ϕ^4 model that poor quality of the pseudorandom numbers used to generate the random fluctuations in the domain walls could lead to unreliable kinetic exponent values. In contrast, the domain-growth kinetics in the $p = 2$ Ising model was found to be insensitive to the quality of the random-number generator used.³³ Milchev *et al.*³³ speculated that the larger configurational phase space of the model with continuous site variables is responsible for the larger sensitivity. It is crucial to note that the computer-simulation study by Milchev *et al.*³³ was carried out by quenching to nonzero temperatures T_f in the ϕ^4 model as well as in the Ising model. In fact, the quench temperatures were close to the critical region. Therefore these authors could argue that the quality of the random numbers is crucial because what is studied in the numerical simulation is the amplification, by *thermal* fluctuations, of the random fluctuations present in the initial unstable system. In the previous studies of soft-wall kinetics yield-

ing $n \simeq \frac{1}{4}$, the quenches were performed at *zero* temperature.⁴⁵ In fact, the models were carefully chosen so as to support domain growth at $T = 0$ in order to avoid difficulties in interpreting data due to the lack of theories accounting for temperature-dependent corrections to dynamical scaling. Furthermore, the systematic study of temperature effects in one of the models, the ($p = 6$)-fold degenerate herringbone model,⁴² demonstrated that finite-temperature effective kinetic exponents could be larger than $\frac{1}{4}$ and in fact close to $n \simeq \frac{1}{2}$ for $T_f \sim 0.5T_c$ in the case of the herringbone model. Recently, van Saarloos and Grant⁴⁶ proposed a reinterpretation of the kinetic data for the soft-wall models and suggested that the peculiar zero-temperature behavior may be replaced by classical-growth kinetics (i.e., $n = \frac{1}{2}$) at finite temperatures. In reply to this suggestion, we showed in a preliminary report^{47,43} that such a crossover indeed takes place.

In the present paper we present the results of an extensive computer-simulation study of the domain-growth kinetics of the two soft-wall models advanced in Refs. 3 and 5. These models are characterized by $p = 2$ and $p = 4$. With reference to the brief discussion above, our results present further evidence that the zero-temperature soft-wall domain-growth kinetics may belong to a separate universality class characterized by a kinetic exponent value of $n \simeq \frac{1}{4}$. For finite temperatures, however, there is a distinct crossover in both models to a different universality class, the one described by the classical exponent value of $n = \frac{1}{2}$. This finding is corroborated by the previously published data for the $p = 6$ soft-wall herringbone model.⁴²

In Sec. II we present the microscopic interaction models on which the present paper is based. The models are anisotropic XY models arrayed on square lattices. The ground states are ($p = 2$)- and ($p = 4$)-fold degenerate, respectively. The principles of thermal quenching by computer simulation are outlined in Sec. III. In Sec. IV results are given for the zero-temperature domain-growth kinetics of the $p = 2$ models as it is monitored by different measures of length scale and interfacial energy. The dynamical structure factor is analyzed and evidence for dynamical scaling is presented. In particular, the kinetic growth law, Eq. (1), is found to hold with $n \simeq 0.25$, independent of the degree of softness of the domain walls. The shape of the walls is demonstrated to be described by a tangent hyperbolic function. The scaling functions pertaining to the structure factor are for large wave vectors shown to comply with a Porod-type law with a decay exponent which is dependent on the softness of the walls. Section V describes the results obtained from quenches to finite temperatures below the ordering transitions. A comparison is provided between soft-wall models with $p = 2, 4$, and 6 . The paper is concluded in Sec. VI by a discussion of soft-wall domain growth kinetics.

II. MODELS

We consider the two classical XY -spin models governed by the Hamiltonians

$$H_1(p=2) = J \sum_{\substack{i,j(i>j) \\ (\text{NNN})}} \cos(\phi_i - \phi_j) - P \sum_{\substack{i,j(i>j) \\ (\text{NN})_x}} \cos\phi_i \cos\phi_j \quad (2)$$

and

$$H_2(p=4) = J \sum_{\substack{i,j(i>j) \\ (\text{NNN})}} \cos(\phi_i - \phi_j) + J \sum_{\substack{i,j(i>j) \\ (\text{NN})_2}} \cos\phi_i \cos\phi_j + J \sum_{\substack{i,j(i>j) \\ (\text{NN})_y}} \sin\phi_i \sin\phi_j - P \sum_i (\cos^4\phi_i + \sin^4\phi_j) \quad (3)$$

with $J > 0$ and $P > 0$. ϕ_i is the polar angle of a classical two-component spin. The models are arrayed on square lattices with next-nearest-neighbor interactions (NNN) and nearest-neighbor interactions (NN) along the x and y axes. The repulsive pair interactions serve to stabilize (2×1) antiferromagnetic ground states with the propagation vector along the sublattice magnetization. In H_1 the P term breaks the cubic symmetry of the (2×1) ordering and singles out the x direction, thus leading to an $n=1$ component Ising-type order parameter. The model is in the static universality class of the two-dimensional Ising model and is expected to have a critical ordering transition with Ising critical exponents. In H_2 the anisotropy induced by the crystal-field-like P term preserves the $n=2$ twofold degenerate (2×1) ordering with discrete symmetry. The model belongs to the static universality class of the planar XY model with cubic anisotropy and is thus expected to have a critical point associated with nonuniversal critical exponents.⁴⁸

At low temperatures, the two models have $p=2$ and $p=4$ thermodynamically degenerate (2×1) antiferromagnetically ordered domains. The two order-parameter components are pictured in Fig. 1. The symmetries of these types of ordering are the same as that of atomic oxygen chemisorbed on the (112) and (110) surfaces of tungsten.⁴⁹⁻⁵¹

Due to the continuous nature of the planar spin variables of the models, the walls which may be formed between different types of ordered domains have a finite

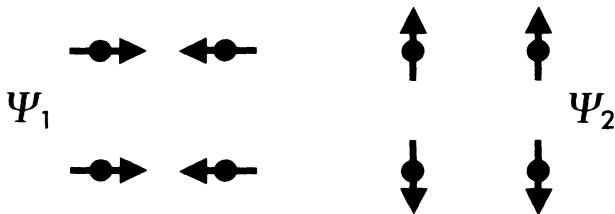


FIG. 1. (2×1) antiferromagnetic ordering on a square lattice. ψ_1 and ψ_2 are degenerate order-parameter components for the $p=4$ model, Eq. (3), and ψ_1 is the one-component order parameter of the $p=2$ model, Eq. (2).

thickness, i.e., the walls are *soft* and they mediate a smooth gradient of the order parameter across the domain boundaries. The P terms of both models control the width and softness of the walls: The smaller the value of P/J , the softer and wider are the walls. In the limit of large P/J , both models become hard-wall models of discrete single-site variables, $\phi_i \simeq 0, \pi$. We shall not be concerned with this limit here, but restrict ourselves to finite and moderate values of the softness parameter P/J .

III. COMPUTER SIMULATION OF THERMAL QUENCHING

The temporal evolution of the ordering process is constructed by Monte Carlo computer simulation⁵² using a Glauber-type single-site excitation mechanism according to the Metropolis algorithm.⁵³ In most runs, the spins are visited at random, and in each attempted excitation the spin is rotated through a random angle. In some runs, the spins are visited sequentially. By the Glauber excitation mechanism, the order parameter is a nonconserved quantity. The initial configuration is chosen as random corresponding to an initial temperature of $T_i \simeq \infty$. The system is then assigned a new temperature, T_f , and the time evolution is followed on a scale given in units of Monte Carlo steps per spin (MCS/S). The simulations are carried out on finite lattices, with $N = L \times L$ spins, subject to toroidal periodic boundary conditions. Finite-size effects are considered by simulation on a series of different lattice sizes, $N = 100^2, 200^2, 300^2$, and 500^2 . Ensemble averages at each time are obtained by averaging over several independent quenches using different random-number sequences. The random numbers used for the present work have been checked very carefully in order to avoid problems of the sort discussed by Milchev *et al.*³³

The growth process is followed in time by several methods. Snapshots of microconfigurations provide a qualitative overall picture of the evolving domain pattern and are useful to gauge the topology of the domain-boundary network and the morphology of the domains. More quantitative measures of the growth use the dynamical structure factor calculated along the modulated directions, e.g., for the $p=2$ model

$$S(q, t) = N^{-1} \left\langle \left| \sum_{j=1}^N \cos[\phi_j(t)] e^{i(q-\pi)r_j} \right|^2 \right\rangle \quad (4)$$

with Bragg condition $q=0$. From the moments of $S(q, t)$

$$k_m(t) = \sum_q |q|^m S(q, t) / \sum_q S(q, t), \quad (5)$$

where $q = 2\pi j/\sqrt{N}$, $j = -\sqrt{N}/2, \dots, 0, \dots, \sqrt{N}/2$ measures of length can be obtained, e.g., as $k_1^{-1}(t)$ and $k_2^{-1/2}(t)$. Another measure of length is the average linear domain size, $R(t)$, derived directly from the domain-distribution function, assuming that $R(t)$ scales as the square root of the domain area. For low values of p , the domain pattern is highly percolative and $R(t)$ becomes a less reliable length measure. From the intensity

of the structure factor at the Bragg condition yet another length scale, $L(t)$, may be obtained,

$$L(t) = [N^{-1}S(0,t)]^{1/2} / \psi(T_f), \quad (6)$$

where $\psi(T_f)$ is the equilibrium value of the order parameter at T_f . Since $L(t)$ is determined by the degree of symmetry breaking between the different ground-state domains, it is subject to large fluctuations from quench to quench.^{9,13,54} It is therefore difficult to estimate $L(t)$, in particular for small values of p . A final length-scale measure is obtained from the excess internal energy

$$\Delta E(t) = E(t) - E(T_f) \quad (7)$$

associated with the entire domain-wall network. $E(t)$ is the nonequilibrium energy at time t and $E(T_f)$ is the equilibrium energy. According to a simple scaling argument advanced for sharp-wall Ising models⁵⁵ $\Delta E^{-1}(t)$ has the property of a length scale. We expect this argument to hold for the present soft-wall models as long as the domain-wall thickness is small compared to the size of the domains. It is anticipated that the argument will not remain valid at higher temperatures where thermal excitations broaden the walls to sizes comparable to the domain-wall extension.

Milchev *et al.*³³ have recently pointed out the importance of lack of self-averaging for the kinetics of domain growth. A quantity is said to lack self-averaging if the statistical error pertaining to that quantity does not decrease by increasing the system size, N . Examples of such quantities include the length scale $L(t)$ in Eq. (6) which therefore has to be averaged over a substantial sample of different quenches in order to reduce the fluctuations. However, a number of quantities are self-averaging, e.g., $\Delta E(t)$, $R(t)$, and the moments of the structure factor.³⁹ These quantities can therefore be estimated accurately by studying fewer quenches on larger systems. The results of the present paper are obtained using $\Delta E^{-1}(t)$, $k_1^{-1}(t)$, and $k_2^{-1/2}(t)$ as length-scale measures for which reliable statistics may be gained from samples of the order of ten quenches on large lattices, $N \geq 100^2$. Possible subtle finite-size effects have been in-

vestigated by systematic variation of the lattice size. The simulation results to be reported below are derived by combining data obtained from different system sizes in such a way that the thermodynamic limit is approached. The time evolution is stopped when finite-size effects set in.

The major part of the quench studies to be reported below refer to global quenches. A few selected controlled-growth studies have also been conducted using special initial domain-pattern geometries in order to study domain-shape functions.

IV. ZERO-TEMPERATURE GROWTH

Results for the zero-temperature domain-growth kinetics have previously been reported for the $p=4$ model⁵ for a variety of P/J values and for the $p=2$ model³ in the case of a single value, $P/J=5$. For the $p=4$ model, the growth process was found to be described by Eq. (1) with $n \simeq 0.25$, independent of the domain-wall softness. For the $p=2$ model, the growth process was shown to obey dynamical scaling and the same growth exponent value $n \simeq 0.25$ was found as for the $p=4$ model. The results suggested that the zero-temperature domain-growth kinetics of these soft-wall models is described by a special universality class which is separate from the hard-wall Lifshitz-Allen-Cahn universality class with $n = \frac{1}{2}$. All these results, together with the corresponding results from the wide-wall Potts-model studies,⁴ suggest that at zero temperature the domain-wall softness may be more important than the degeneracy of the ground state for a possible universal classification of domain-growth kinetics.

In this section we give a detailed account of zero-temperature quenching studies for the $p=2$ model for a wide range of P/J values. New results for the $p=4$ model will be reported in Sec. V on finite-temperature growth.

A. Domain growth

In Fig. 2 a series of snapshots is given of the domain-wall network as it evolves in time for the $p=2$ model

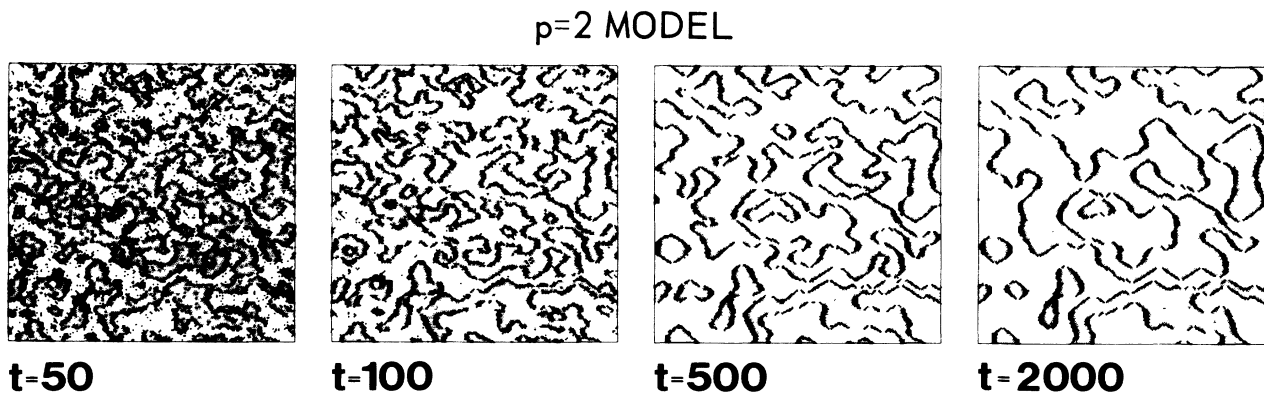


FIG. 2. Zero-temperature domain-wall network at different times t (in units of MCS/S) for the $p=2$ model with $P/J=2$ on a lattice with $N=200^2$ spins. The two ordered ground-state domains are indicated by white and grey regions separated by the black wall spins.

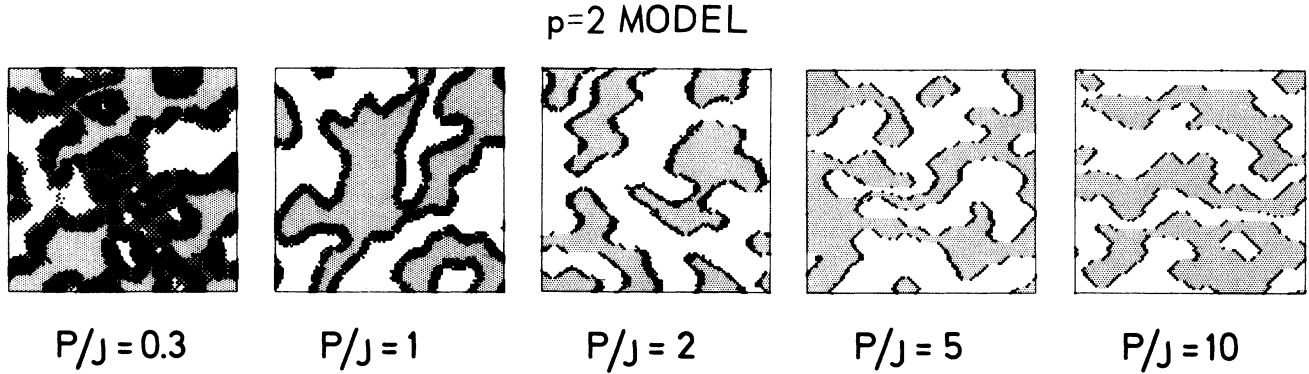


FIG. 3. Snapshots of zero-temperature domain-wall configurations for the $p=2$ model at $t=500$ MCS/S for different values of P/J . The model contains $N=100^2$ spins.

with $P/J=2$. A spin is determined to belong to a wall if its angle deviates more than $\pi/15$ from a ground-state angle.^{5,6} The domain pattern is very ramified and percolative. At very early times a spanning cluster is formed. Still, the domains are compact at small length scales. When p is increased, the boundary-network topology plays a larger role and for $p=4$ and 6 , the domain pattern becomes more regular with vertices.^{6,56} Similar observations have been made for Ising³¹ and Potts models.¹⁸

The late-time domain-wall thickness⁵ as a function of P/J is illustrated qualitatively in Fig. 3. It is seen that the wall thickness decreases as P/J is increased. This is a significant effect, e.g., the wall thickness decreases by an order of magnitude for P/J going from one to ten. In the case of $P/J=0.3$, the limiting domain-wall size has not been reached. Figure 3 reveals another important property of the $p=2$ model: At $T=0$, two types of walls can be discerned—a wide-wall type roughly along the lattice diagonals and a sharp-wall type along the preferred x axis. Having once been formed, the latter wall type will remain infinitely sharp. The distinction between the walls becomes less pronounced as P/J is lowered. An analysis of the wall shape will be presented in Sec. IV D.

It is also seen from Fig. 3 that the larger the value of P/J , the earlier the system develops “slab configurations” which will eventually pin the walls to the lattice and the growth will cease. This is a finite-size effect induced by the periodic boundary conditions and it is similar to that commonly observed in Ising antiferromagnets on square lattices.^{23,24,34} The time at which finite-size slab effects become important is conveniently determined from a systematic comparison between growth data for different system sizes.

B. Structure factors and dynamical scaling

Results for the zero-temperature dynamical structure factor Eq. (4) for the $p=2$ model in the case $P/J=5$ are shown in Fig. 4 for a selected series of times. As time elapses, a peak of increasing intensity is built up around the Bragg condition $q=0$. The width of the structure factor is found to increase when P/J decreases, that is, when the walls soften.

The dynamical scaling properties of the ordering process are studied via the scaling functions

$$F_m(x) = k_m^{2/m} S(q, t), \quad (8)$$

where $x = qk_m^{-1/m}$ is the scaling variable. In Figs. 5 and 6 the scaling functions F_1 and F_2 are given pertaining to the structure factor in Fig. 4. The corresponding F_2 for $P/J=2$ is displayed in Fig. 7. These figures show that the structure-factor data for $T \gtrsim 80$ are accurately described by a single scaling function, be it F_1 or F_2 . Thus the growth process obeys dynamical scaling. At low values of $|q|$ we are unable to perform a critical test of dynamical scaling. The reason for this is that the individual structure factors, of which the average in Fig. 4 is composed, have very complicated patterns of peaks due to scattering from the inhomogeneous random-domain-wall networks.³ The averaging requires more statistics the smaller the value of the wave vector $|q|$. The low-

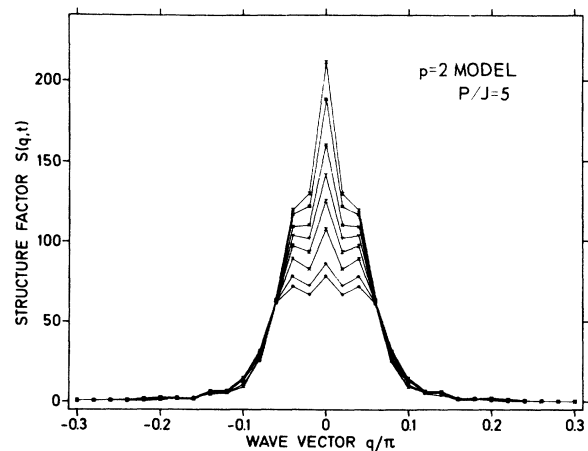


FIG. 4. Zero-temperature dynamical structure factor $S(q, t)$, Eq. (4), for the $p=2$ model with $P/J=5$ calculated at times $t=80, 100, 150, 200, 250, 300, 400,$ and 500 for a system with $N=100^2$ spins. The curves appear from bottom to top as t is increased. All possible wave vectors ($q \leq 0.3\pi$) in the first Brillouin zone are displayed.

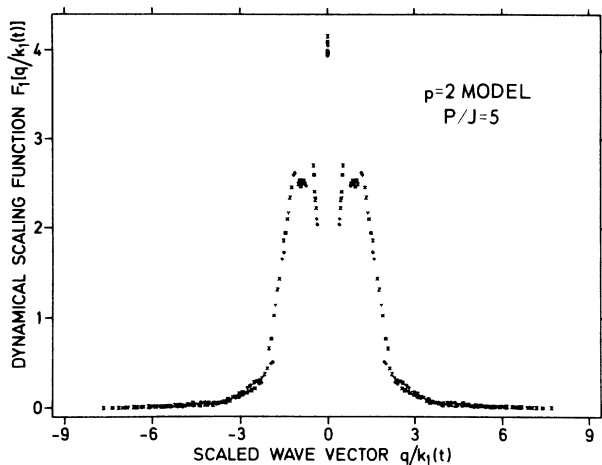


FIG. 5. Zero-temperature dynamical scaling function $F_1(x)$, Eq. (8), derived from the structure factor in Fig. 4 for the $p=2$ model with $P/J=5$.

$|q|$ shoulder and the scattering at $q=0$ are thus caused by incomplete averaging. Moreover, the nonsmooth behavior at low $|q|$ may also be influenced by metastable slab effects²¹ which have the major weight on large-scale properties, i.e., close to the Bragg condition. Similar difficulties at low $|q|$ have been reported for a number of other growth models.^{21,23–25,28,29,44,57} These findings underscore our choice of length-scale measures discussed in Sec. III as measures which give weight to nonzero wave-vector components of the structure factor. In fact it is found, for example, that k_1 and k_2 are only slightly sensitive to the detailed satellite pattern of the individual structure factors and thus remain good self-averaging properties.

A comparison of Figs. 6 and 7 shows that the scaling functions depend on the value of the softness parameter P/J : The softer the walls, the wider the scaling func-

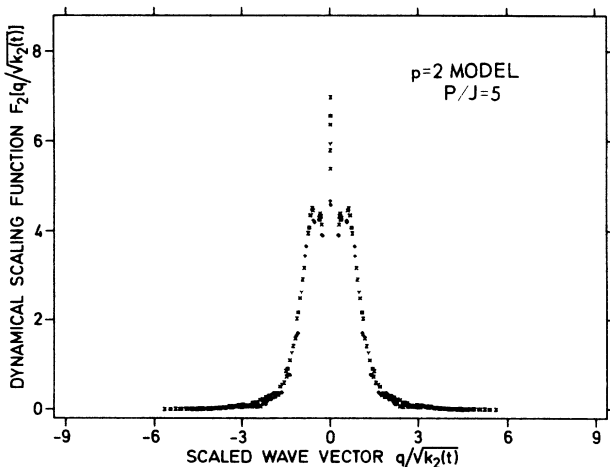


FIG. 6. Zero-temperature dynamical scaling function $F_2(x)$, Eq. (8), derived from the structure factor in Fig. 4 for the $p=2$ model with $P/J=5$.

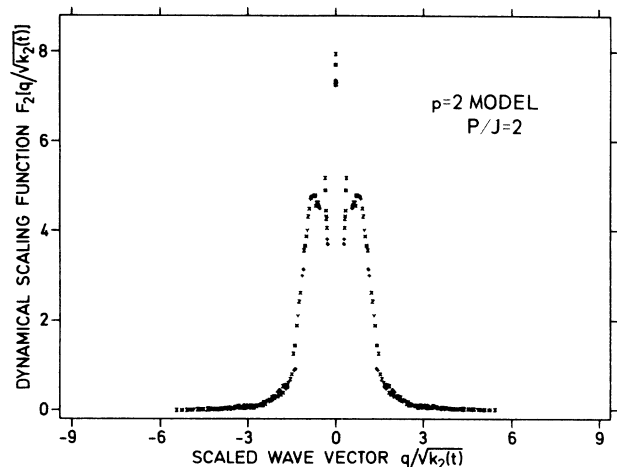


FIG. 7. Zero-temperature dynamical scaling function $F_2(x)$, Eq. (8), for the $p=2$ model with $P/J=2$. The data are obtained from a system with $N=100^2$ spins.

tions. A quantitative discussion is given in Sec. IV F in terms of Porod-law behavior of the large- $|q|$ decay of the scaling functions and its dependence of P/J . It is noteworthy that we find such model-parameter dependences of the scaling functions for the soft-wall models. For a number of hard-wall models the scaling functions were found to be insensitive to details of the model.^{21,36,57}

C. The growth law

The existence of a scaling function, Eq. (8), as confirmed by Figs. 5–7 implies that the growth process is characterized by a single length scale. It is usually assumed that this length scale varies algebraically in time,

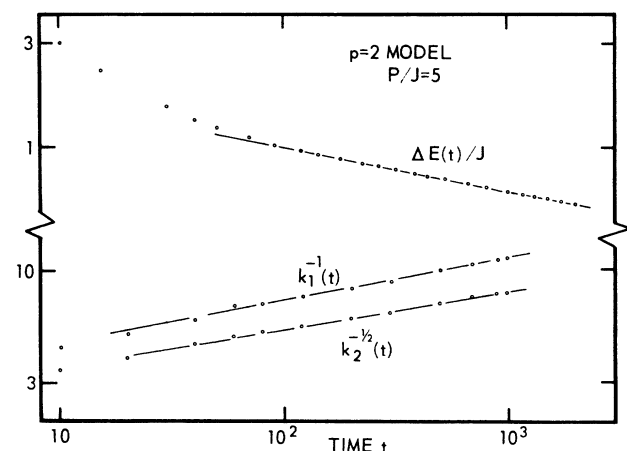


FIG. 8. Zero-temperature growth data for the $p=2$ model in the case $P/J=5$. Results are given for excess energy $\Delta E(t)$ and appropriate powers of the two first moments $k_1(t)$ and $k_2(t)$ of the dynamical structure factor. The solid lines indicate the power laws, Eq. (9), with $n \approx 0.25$. The bulk of the data refers to a system of size $N=300^2$.

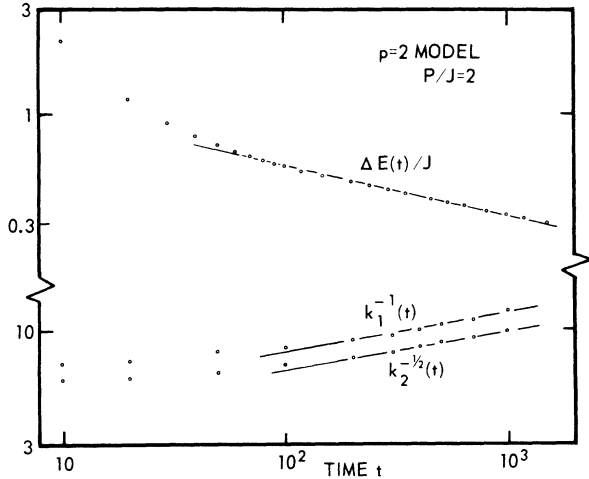


FIG. 9. Zero-temperature growth data for the $p = 2$ model in the case $P/J = 2$. The bulk of the data is derived from a system of size $N = 500 \times 500$. The solid lines are the power laws, Eq. (9), with $n \simeq 0.25$.

Eq. (1). For our particular measures of length, Eq. (1) reads

$$k_1^{-1}(t) \sim k_2^{-1/2}(t) \sim \Delta E^{-1}(t) \sim t^n. \quad (9)$$

The data in Fig. 8 demonstrate that for $P/J = 5$ such algebraic growth laws indeed describe our late-time data with a high degree of accuracy. The common exponent value is $n \simeq 0.25$. For a given lattice size, the growth in the present $p = 2$ soft-wall model may be followed to considerably later times than in corresponding $p = 2$ Ising models.²⁴ This is due to the much faster growth kinetics ($n = \frac{1}{2}$) of the nonconserved Ising models.

Growth data for a smaller value of the softness parameter $P/J = 2$ are given in Fig. 9. Again we find that the data at late times may be constrained to the power laws, Eq. (9), with the same exponent value, $n \simeq 0.25$ as obtained for $P/J = 5$. The full variation of the effective

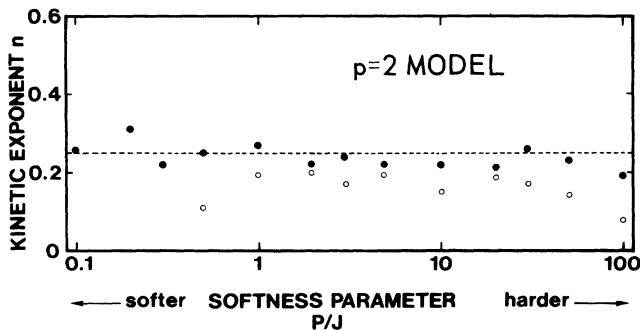


FIG. 10. Effective zero-temperature growth exponents derived for the $p = 2$ model as a function of softness parameter P/J . The different symbols refer to the exponent values for the excess energy (\bullet) and for the structure factor moments (\circ). The horizontal dashed line indicates $n = 0.25$. Note that the horizontal axis is logarithmic.

growth exponent as a function of P/J over a substantial range is displayed in Fig. 10. The exponent values derived from the excess energy and the structure-factor moments are displayed separately. The data points scatter in the neighborhood of $n = 0.25$ with a tendency for the exponent values derived from the moments to fall slightly below those derived from excess energy. The scatter in the points reflects the accuracy of the exponent determination from the raw growth data, the accuracy in turn being dictated by the statistics available. The points at $P/J = 2$ and 5 are based on the most comprehensive statistics and should therefore be considered the most reliable. It is noticeable that for large P/J , the effective exponent values have a decreasing trend. In line with the previously discussed finite-size effects, this trend is caused by the slab effects which slow down the growth at earlier times as the walls get harder. The system presumably loses its connectivity for the largest values of P/J studied and effectively behaves as a one-dimensional system. Consequently, the data displayed in Fig. 10 for the largest P/J values should not be considered as representing the true late-time behavior for the present model. A similar situation of crossover to zero-temperature hard-wall pinned behavior was encountered for the $p = 4$ model.⁵ The data in Fig. 10 strongly suggest that the characteristic zero-temperature growth exponent for the $p = 2$ model is close to $n = 0.25$, independent of the softness parameter. This indicates that a universal principle is operative. An exponent value of $n \simeq 0.20$ is also consistent with the available data.

D. Controlled growth and domain-wall shapes

It is difficult to extract a quantitative measure of the domain-wall thickness for the $p = 2$ model with the very convoluted domain patterns obtained by global quenching. In contrast, this can be readily done for the more compact domain structures occurring in models with higher p , simply by combining information on the total perimeter from the domain-size distribution function with the total area of the boundary spins.⁵ For the $p = 2$ model, the domain-wall thickness should rather be extracted from a controlled growth experiment in which a specific interface of a simple geometry is introduced in an ordered structure and then studied at late times.

We study the time evolution of an initially sharp linear interface along the y axis. Such a situation corresponds precisely to a perfect slab configuration. There is no growth, but the interface widens as time elapses and approaches a limiting thickness after a few hundred MCS/S, the precise number depending on P/J . The smaller the value of P/J , the wider is the wall at late times. A presentation of these results is given in Fig. 11 in terms of the spatial variation of the average string magnetization, or order parameter profile,

$$m(r_x) = L^{-1} \sum_{j=1}^L \cos[\phi_j(r_x)] e^{i(q-\pi)r_x} \quad (10)$$

calculated across the domain-wall center at $r_x = 0$. The coordinate r_x is measured in units of the lattice constant. It turns out that the order-parameter profile can be fitted

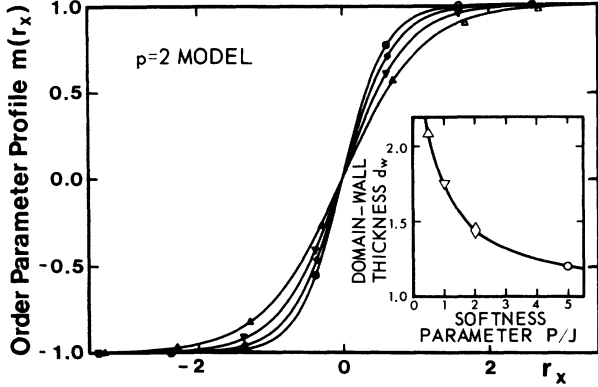


FIG. 11. Order-parameter profile $m(r_x)$, Eq. (10), across the domain wall for the $p=2$ model at zero temperature for various softness parameter values: $P/J = \frac{1}{2}$ (\triangle), 1 (∇), 2 (\diamond), and 5 (\circ). The solid lines are the fitted tanh shape functions, Eq. (11). The inset shows the domain-wall thickness d_w vs P/J as derived from the shape functions.

very accurately to the hyperbolic shape function

$$m(r_x) = \tanh(2r_x/d_w), \quad (11)$$

where d_w is a measure of the thickness of the domain wall. Thus the shape of the wall is the same as that resulting from a simple Landau-Ginzburg analysis of the free energy of a domain wall.^{22,58} Using d_w as a measure of the domain-wall thickness, it seems justified to assume that the wall thickness is much smaller than the average linear domain size in the time regime where the growth exponent is extracted. Thus there is only one relevant length scale in the present growth problem.

E. Porod's law

It is of interest to analyze the high- $|q|$ tail of the structure factor (or the dynamical scaling function) since this tail contains information on short-distance structure of the domain pattern. Furthermore, the tail is accessible in a low-angle scattering experiment.⁵⁹ We shall here show that the shape of this tail depends on the domain-wall softness and thus may be used to distinguish domain-boundary networks with soft and hard walls.

Figure 12 gives a composite log-log plot of the dynamical scaling functions $F_2(x)$ of Figs. 6 and 7 for $P/J=5$ and 2, respectively. There is considerable scatter in the data in this representation. However, it is clear that for $x \gtrsim 0.4$ the data in both cases may be described by a Porod-type law

$$F_2(x) \sim x^{-\omega} \quad (12)$$

with decay exponents $\omega \simeq 3.6$ for $P/J=5$ and $\omega \simeq 3.9$ for $P/J=2$. The same statement and the same values of ω apply for $F_1(x)$. General arguments on scaling in the dynamics of random sharp interfaces¹⁰ predict a Porod law for the scaling function with decay exponent $\omega = d + 1$, where d is the spatial dimension. This prediction is in accordance with a number of computer-simulation studies

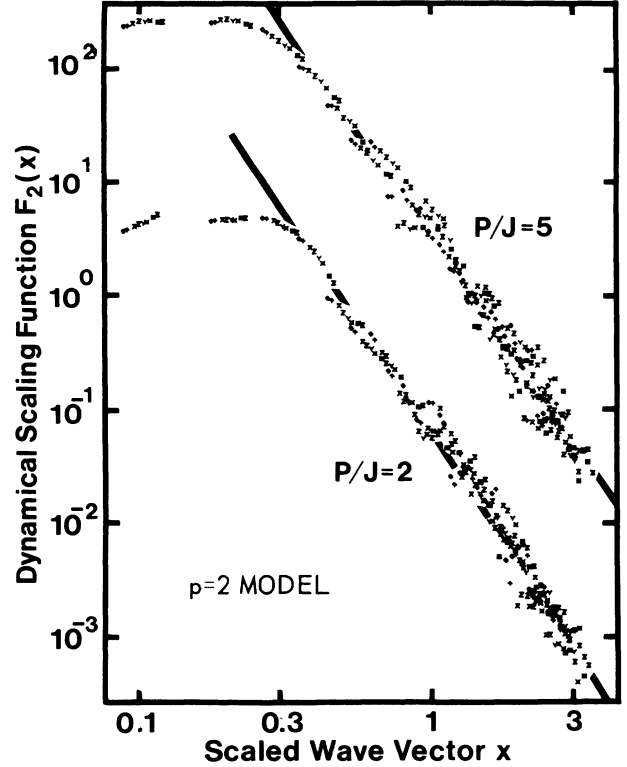


FIG. 12. Log-log plot of the zero-temperature dynamical scaling functions $F_2(x)$, Figs. 6 and 7, for the $p=2$ model in the cases $P/J=5$ and 2. The data for $P/J=5$ are shifted upwards for the sake of clarity. The solid lines denote the Porod law, Eq. (12), with decay exponents $\omega = 3.6$ and 3.9 for $P/J=5$ and 2, respectively.

of hard-wall Ising models.^{9,21,23,27,36,60}

Two important conclusions can be drawn: (i) the Porod law is a good description of the large- $|q|$ decay of the dynamical scaling function for both models with hard- and soft-domain walls, and (ii) the decay exponent ω is larger for the soft-wall systems than for the hard-wall systems and ω increases as the walls become softer. It is interesting to note that an analysis of the scaling function for another soft-wall model, the $p=6$ herringbone model,⁶¹ is consistent with a Porod law with $\omega \simeq 3.3$. This value is quite reasonable since the herringbone domain walls are softer than the Ising walls, but harder than the walls of the $p=2$ model with $P/J=2$.⁵

V. FINITE-TEMPERATURE GROWTH

In this section we present the results of quenches of both the $p=2$ model and the $p=4$ model from infinite temperature to temperatures $T_f > 0$ below the ordering transition temperature. Only a single value of P/J has been considered for each model. The critical temperatures T_c , as well as the equilibrium energy data necessary for a determination of the excess energy, Eq. (7), have been calculated by standard equilibrium Monte Carlo techniques.⁵² Only quenches to temperatures well below T_c , $\tau = T_f/T_c < 0.7$, have been considered. There are

several reasons for this. First, we want to avoid effects due to critical fluctuations,^{2,34} second, our main purpose is to reveal possible crossover effects from zero-temperature to finite-temperature growth kinetics; and third, the scaling assumption⁵⁵ which relates $\Delta E^{-1}(t)$ to a length scale (the perimeter) breaks down at higher temperatures where thermal excitations have blurred the walls. The last difficulty is also encountered in studies of hard-wall Ising and Potts models, although somewhat closer to the transition.^{2,34}

The results for the finite-temperature growth kinetics presented in the present section are discussed in Sec. VI together with previously published data for the finite-temperature growth in the soft-wall $p=6$ herringbone model.

A. $p=2$ model

Figure 13 presents results for $\Delta E(t)$ from selected finite-temperature quenches of the $p=2$ model with $P/J=5$. The set of data for quench temperatures up to $\tau=T_f/T_i \approx 0.1$ shows a gradual increase in the effective late-time kinetic exponent towards a limiting value of $n \approx 0.50$. For $\tau \geq 0.1$ n remains constant around this value. Figure 13 reflects the fact that the higher the temperature is, the shorter timespan can be investigated for a given system size before finite-size effects set in. A similar crossover in kinetic exponent value as a function of temperature is observed for the length scales derived from the moments of the structure function. However, the data for the moments are more strongly influenced by the thermal fluctuations and consequently subject to larger statistical fluctuations than the excess energy. The data in Fig. 13 do not reveal a well-defined crossover region from some early-time behavior (possibly influenced by the zero-temperature kinetic behavior) to a distinct Lifshitz-Allen-Cahn law at later times. It is likely that such a crossover region exists but the data are not sufficiently accurate to localize it. In this respect the $p=2$ model is different from the $p=4$ model as shown in the following subsection.

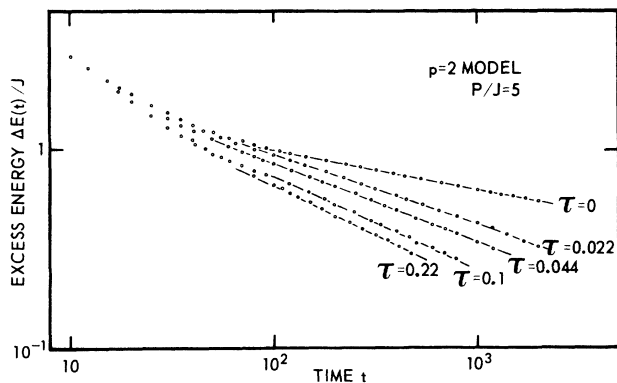


FIG. 13. Finite-temperature domain-growth data for the $p=2$ model with $P/J=5$. $\Delta E(t)$ vs time is shown for a series of selected temperatures $\tau=T_f/T_c$. The solid lines denote the effective growth laws with the corresponding effective growth exponents given in Fig. 15.

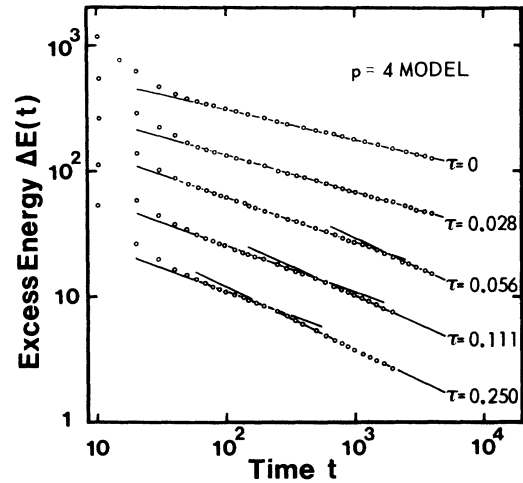


FIG. 14. Finite-temperature domain-growth data for the $p=4$ model with $P/J=2$. $\Delta E(t)$ vs time is shown for a series of reduced temperatures $\tau=T_f/T_c$. The data refer to a system with $N=100^2$ spins. The solid lines denote the effective growth laws, and the corresponding effective growth exponents are given in Fig. 15. The various sets of data have been shifted along the vertical axis for the sake of clarity.

B. $p=4$ model

The excess energy versus time resulting from a series of finite-temperature quenches of the $p=4$ model with $P/J=2$ is shown in Fig. 14. The following striking observations can be made from this figure: As the temperature is raised above zero, a distinct crossover in the kinetic behavior sets in. A characteristic crossover region around a time t_c can be identified which separates the

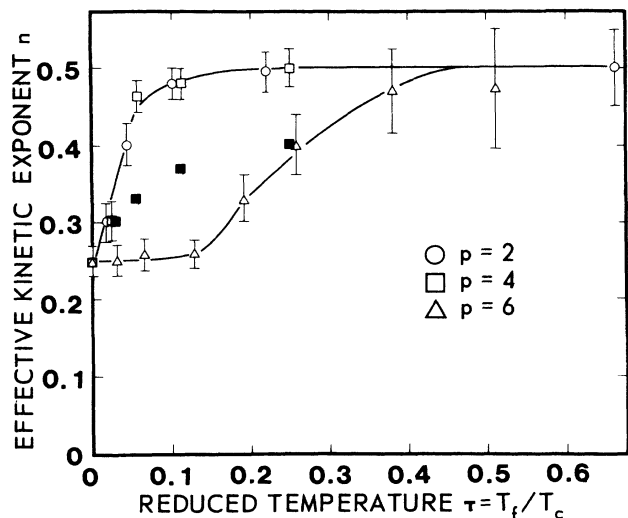


FIG. 15. Plot of effective growth exponents vs reduced quench temperature $\tau=T_f/T_c$ for the $p=2$ model (Fig. 13), the $p=4$ model (Fig. 14), and the $p=6$ herringbone model (Ref. 42). The open symbols for the $p=2$ and $p=4$ models refer to the late-time kinetics, and the solid symbols for the $p=4$ model refer to the early-time kinetics. For the sake of clarity, error bars on the early-time exponents have been omitted.

early-time kinetics from the late-time behavior. The crossover time t_c decreases as the temperature is increased, e.g., $t_c > 2000$, $\simeq 1500$, $\simeq 600$, and $\simeq 200$ for $\tau = T_f/T_c = 0.028$, 0.056 , 0.111 , and 0.250 , respectively. Each of the regions $50 < t < t_c$ and $t > t_c$ can be characterized by its own effective kinetic exponent as indicated by the solid lines in Fig. 14. These exponents are compiled in Fig. 15. The late-time exponents are found to rise very steeply towards $n = 0.50$ as the temperature gets finite. The early-time exponent displays a much slower increase. For the two highest temperatures it is not possible to follow the evolution of the system beyond $t \sim 2000$ due to finite-size effects in the $N = 100^2$ system. For the same reason, only quench temperatures up to $\tau = 0.25$ have been considered for the $p = 4$ model.

VI. DISCUSSION: SOFT-WALL DOMAIN-GROWTH KINETICS

We have in this paper presented strong numerical evidence for a special *zero-temperature* kinetic behavior of the domain growth in two-dimensional anisotropic XY models which are characterized by their capacity of supporting soft-domain walls. The zero-temperature kinetics is described by a growth exponent value, $n \simeq 0.25$, which is distinctly lower than the classical Lifshitz-Allen-Cahn value of $n = \frac{1}{2}$ for nonconserved order parameter. The ordering in the models is twofold and fourfold degenerate, respectively. Exponent values of 0.25 are also found for the sixfold degenerate soft-wall herringbone model^{6,42} and for the wide-wall limit of 48-fold-degenerate anisotropic Potts models.⁴ All these results suggest that at zero temperature the soft-wall domain-growth kinetics belongs to a separate universality class. Moreover, it is found that it is not the softness as such, or how soft the walls actually are, which influences the growth, but rather the potential of the walls to soften, in particular to soften locally in response to interfacial curvature.

At *finite temperatures* however, a distinct crossover is found to a domain-growth kinetics which is well described by the Lifshitz-Allen-Cahn law. This is clearly demonstrated by Fig. 15 for the $p = 2$, $p = 4$, and $p = 6$ models. The wide-wall Potts models with $p = 48$ have only been studied at zero temperature, and it would be interesting to extend the study to finite temperatures in order to see whether the Lifshitz-Allen-Cahn exponent is recovered for this model as well. Figure 15 shows that the crossover to $n \simeq 0.50$ is very fast and proceeds in a similar manner for the $p = 2$ and $p = 4$ models. For the $p = 4$ model, an early-time effective exponent may be discerned which rises slowly with temperature. This early-time exponent could be considered a weighted average of the zero-temperature exponent $n \simeq 0.25$ and the finite-temperature exponent $n \simeq 0.50$. This behavior is possibly described by some kind of crossover scaling function. For the $p = 6$ herringbone model, the crossover to $n \simeq 0.50$ is considerably slower, and it cannot be excluded that the value $n \simeq 0.25$ may apply to a range of low temperatures. Excluding this latter possibility, however, a coherent picture of the three soft-wall models appears. This picture may conveniently be expressed in the

language of renormalization-group studies of domain growth.^{20,30,62,63} At zero temperature, the growth is governed by a stable equilibrium fixed point characterized by the exponent value $n \simeq 0.25$. At finite temperatures this fixed point becomes unstable and the growth is then governed by another stable equilibrium fixed point characterized by the classical exponent $n = \frac{1}{2}$. At short times and at low temperatures one observes temperature-dependent effective exponents due to crossover between the two fixed points, cf. Fig. 15.

Recently, a couple of papers have appeared which have questioned the proposal of a separate soft-wall universality class for domain-growth kinetics.^{33,46,64} We shall here address some of the points in dispute. First, the finding of Milchev *et al.*³³ of the Lifshitz-Allen-Cahn exponent for the $p = 2$ φ^4 model refers to finite temperatures and is hence in full accordance with our results.⁴⁷ It would be interesting to study the growth kinetics of the φ^4 model at zero temperature to see if there is a crossover to $n \simeq 0.25$. Second, and along the same lines, it is interesting to note that our finite-temperature results are also consistent with the finding of Lifshitz-Allen-Cahn kinetics in the finite-temperature electric-field quenching experiments on smectic films by Pindak *et al.*⁶⁵ These experimental results which, as pointed out by van Saarloos and Grant,⁴⁶ appear to have been overlooked in the field of domain-growth kinetics, refer to a situation with continuous single-particle variables being the director angles of the molecular electric dipoles of the liquid crystal. These dipoles can support soft-domain walls of a thickness which is found to vary with the applied electric quenching field.⁶⁵ Interestingly enough, the experiments show that the kinetic exponent value is independent of the actual width of the walls. Finally, van Saarloos and Grant⁴⁶ have argued that the soft-wall results at zero temperature³ may suffer from a $\ln t$ rescaling of the time scale due to the particular Monte Carlo algorithm used at zero temperature. As we have recently pointed out,⁴⁷ this rescaling is likely to apply only in the one-dimensional limit ($J = 0$) of the model, Eq. (2), which these authors consider in their calculation. This special limit corresponds to the particular two-dimensional linear-wall geometries considered in Sec. IV D. For these geometries, which are essentially the slab configurations slowing down the growth, only a wall-widening process is observed. Consequently, the next-nearest-neighbor interactions absent in the $J = 0$ limit are essential for the domain-wall motions observed in the full two-dimensional $p = 2$ model.

An unsolved question remains regarding the mechanism which underlies the special zero-temperature domain-growth kinetics of systems with soft walls. A possible key to answering this question may be found in the observation⁴⁷ made from direct inspection of snapshots of domain-wall networks like those in Fig. 2, that growth proceeds partially via soft-wall formation. Specifically, it is found that in regions with high local curvature, the walls not only move, but also soften. This effectively leads to a slowing down of the growth rate and could possibly imply a breakdown of the basic assumption underlying the Allen-Cahn theory⁸ regarding the inverse proportionality of wall width and interface tension.

ACKNOWLEDGMENTS

Gary Grest is thanked for very useful discussions on general aspects of domain-growth kinetics. Some helpful remarks by David Landau are greatly appreciated. We are grateful to Jim Gunton who provided us with the numerical data for the herringbone dynamical structure factor of Ref. 61. Wim von Saarloos and Martin Grant are

acknowledged for sending us before publication their work criticizing our previous work on domain-growth kinetics of systems with soft walls. The major part of the calculations in this paper were performed at the Computing Center at Roskilde University and we wish to thank Jan Andersen for assistance with the computations. This work was supported by the Danish Natural Science Council under Grant J. nr. 5.21. 99.72.

- ¹For a review, see J. D. Gunton, M. San Miguel, and P. S. Sahni, in *Phase Transitions and Critical Phenomena*, edited by C. Domb and J. L. Lebowitz (Academic, New York, 1983), Vol. 8, p. 269.
- ²A. Sadiq and K. Binder, *Phys. Rev. Lett.* **51**, 674 (1983); *J. Stat. Phys.* **35**, 517 (1984).
- ³O. G. Mouritsen, *Phys. Rev. Lett.* **56**, 850 (1986).
- ⁴G. S. Grest, D. J. Srolovitz, and M. P. Anderson, *Phys. Rev. Lett.* **52**, 1321 (1984).
- ⁵O. G. Mouritsen, *Phys. Rev. B* **31**, 2631 (1985).
- ⁶O. G. Mouritsen, *Phys. Rev. B* **28**, 3150 (1983).
- ⁷I. M. Lifshitz, *Zh. Eksp. Teor. Fiz.* **42**, 1354 (1962) [*Sov. Phys.—JETP* **15**, 939 (1962)].
- ⁸S. A. Allen and J. W. Cahn, *Acta. Metall.* **27**, 1085 (1979).
- ⁹G. F. Mazenko and O. T. Valls, *Phys. Rev. B* **30**, 6732 (1984).
- ¹⁰T. Ohta, D. Jasnow, and K. Kawasaki, *Phys. Rev. Lett.* **49**, 1223 (1982).
- ¹¹H. Tomita, *Prog. Theor. Phys.* **75**, 482 (1986).
- ¹²M. Grant and J. D. Gunton, *Phys. Rev. B* **28**, 5496 (1983).
- ¹³G. F. Mazenko and O. T. Valls, *Phys. Rev. B* **27**, 6811 (1983).
- ¹⁴P. A. Rikvold and J. D. Gunton, *Phys. Rev. Lett.* **49**, 286 (1982).
- ¹⁵P. W. Voorhees, *J. Stat. Phys.* **38**, 231 (1985).
- ¹⁶S. A. Safran, *Phys. Rev. Lett.* **46**, 1581 (1981).
- ¹⁷H. Furukawa, *Phys. Rev. A* **30**, 1052 (1984).
- ¹⁸P. S. Sahni, D. J. Srolovitz, G. S. Grest, M. P. Anderson, and S. A. Safran, *Phys. Rev. B* **28**, 2705 (1983).
- ¹⁹G. S. Grest, M. P. Anderson, and D. J. Srolovitz, in *Time-Dependent Effects in Disordered Materials*, edited by R. Pynn (Plenum, New York, 1987), p. 365.
- ²⁰J. Viñals and J. D. Gunton, *Phys. Rev. B* **33**, 7795 (1986).
- ²¹S. Kumar, J. D. Gunton, and K. K. Kaski, *Phys. Rev. B* **35**, 8517 (1987).
- ²²S. A. Safran, P. S. Sahni, and G. S. Grest, *Phys. Rev. B* **28**, 2693 (1983).
- ²³P. S. Sahni, G. Dee, J. D. Gunton, M. Phani, J. L. Lebowitz, and M. Kalos, *Phys. Rev. B* **24**, 410 (1981).
- ²⁴K. Kaski, M. C. Yalabik, J. D. Gunton, and P. S. Sahni, *Phys. Rev. B* **28**, 5263 (1983).
- ²⁵T. Ala-Nissila, J. D. Gunton, and K. Kaski, *Phys. Rev. B* **33**, 7583 (1986); K. Kaski, T. Ala-Nissila, and J. D. Gunton, *ibid.* **31**, 310 (1985).
- ²⁶G. F. Mazenko, O. T. Valls, and F. C. Zhang, *Phys. Rev. B* **31**, 4453 (1985).
- ²⁷F. C. Zhang, O. T. Valls, and G. F. Mazenko, *Phys. Rev. B* **31**, 1579 (1985).
- ²⁸J. Viñals and J. D. Gunton, *Surf. Sci.* **157**, 473 (1985).
- ²⁹P. S. Sahni and J. D. Gunton, *Phys. Rev. Lett.* **47**, 1754 (1981).
- ³⁰S. Kumar, J. Viñals, and J. D. Gunton, *Phys. Rev. B* **34**, 1908 (1986).
- ³¹G. S. Grest and D. J. Srolovitz, *Phys. Rev. B* **30**, 5150 (1984).
- ³²E. T. Gawlinski, M. Grant, J. D. Gunton, and K. Kaski, *Phys. Rev. B* **31**, 281 (1985).
- ³³A. Milchev, K. Binder, and D. W. Heermann, *Z. Phys. B* **63**, 521 (1986); see also, O. T. Valls and G. F. Mazenko, *Phys. Rev. B* **34**, 7941 (1986) for a study of the ϕ^4 model via the Langevin equation.
- ³⁴A. Høst-Madsen, P. J. Shah, T. V. Hansen, and O. G. Mouritsen, *Phys. Rev. B* **36**, 2333 (1987).
- ³⁵G. F. Mazenko and O. T. Valls, *Phys. Rev. B* **33**, 1823 (1986).
- ³⁶H. C. Fogedby and O. G. Mouritsen, *Phys. Rev. B* **37**, 5962 (1988).
- ³⁷J. D. Gunton, in *Time-Dependent Effects in Disordered Materials*, Ref. 19, p. 387.
- ³⁸D. A. Huse, *Phys. Rev. B* **34**, 7845 (1986).
- ³⁹J. G. Amar, F. E. Sullivan, and R. D. Mountain, *Phys. Rev. B* **37**, 196 (1988).
- ⁴⁰See also, G. F. Mazenko and O. T. Valls, *Phys. Rev. Lett.* **59**, 680 (1987).
- ⁴¹We refer in this paper to Eq. (1) with $n = \frac{1}{2}$ as the Lifshitz-Allen-Cahn growth law despite the fact that the theory of Lifshitz (Ref. 7) and that of Allen and Cahn (Ref. 8) assume different types of driving forces for the interface motions. Both theories lead, however, to the same value of n although the prefactors of the growth law are different.
- ⁴²O. G. Mouritsen, *Phys. Rev. B* **32**, 1632 (1985).
- ⁴³O. G. Mouritsen, H. C. Fogedby, and E. Praestgaard, *Dynamics of Ordering Processes in Condensed Matter*, (Plenum, New York, in press)
- ⁴⁴For an alternative interpretation of the results in Ref. 6, see K. Kaski, S. Kumar, J. D. Gunton, and P. A. Rikvold, *Phys. Rev. B* **29**, 4420 (1984).
- ⁴⁵The quenches of the wide-wall Potts models of Ref. 4 were also performed at zero temperature.
- ⁴⁶W. van Saarloos and M. Grant, *Phys. Rev. B* **37**, 2274 (1988).
- ⁴⁷O. G. Mouritsen and E. Praestgaard, *Phys. Rev. B* **37**, 2278 (1988).
- ⁴⁸E. Domany and E. K. Riedel, *Phys. Rev. Lett.* **40**, 561 (1978).
- ⁴⁹G.-C. Wang and T.-M. Lu, *Phys. Rev. Lett.* **50**, 2014 (1983).
- ⁵⁰M. C. Tringides, P. K. Wu, and M. G. Lagally, *Phys. Rev. Lett.* **59**, 315 (1987).
- ⁵¹P. K. Wu, J. H. Perpezko, J. T. McKinney, and M. G. Lagally, *Phys. Rev. Lett.* **51**, 1577 (1983).
- ⁵²O. G. Mouritsen, *Computer Studies of Phase Transitions and Critical Phenomena* (Springer, Heidelberg, 1984).
- ⁵³D. W. Heermann, *Computer Simulation Methods* (Springer, Heidelberg, 1986).
- ⁵⁴G. S. Grest and D. J. Srolovitz, *Phys. Rev. B* **32**, 3014 (1985).
- ⁵⁵K. Binder and D. Stauffer, *Phys. Rev. Lett.* **33**, 1006 (1974).
- ⁵⁶O. G. Mouritsen, in *Annealing Processes—Recovery, Recry-*

- stallization, and Grain Growth*, Proceedings of the 7th Risø International Symposium on Metallurgy and Materials Science, Risø, 1986, edited by N. Hansen, D. J. Jensen, T. Leffers, and B. Ralph (Risø National Laboratory, Roskilde, 1986), p. 457.
- ⁵⁷K. Kaski, J. Nieminen, and J. D. Gunton, *Phys. Rev. B* **31**, 2998 (1985).
- ⁵⁸J. S. Langer, *Ann. Phys. (N.Y.)* **65**, 53 (1971).
- ⁵⁹P. Porod, in *Small Angle X-Ray Scattering*, edited by O. Glatter and O. Kratsky (Academic, New York, 1982), p. 17.
- ⁶⁰For corrections to Porod's law, see e.g., H. Tomita, *Prog. Theor. Phys.* **75**, 482 (1986); S. Kumar, J. D. Gunton, and K. K. Kaski, *Phys. Rev. B* **35**, 8517 (1987).
- ⁶¹K. Kaski, B. Kumar, J. D. Gunton, and P. A. Rikvold, *Surf. Sci.* **152**, 859 (1985); *Phys. Rev. B* **29**, 4420 (1984).
- ⁶²J. Viñals, M. Grant, M. San Miguel, J. D. Gunton, and E. T. Gawlinski, *Phys. Rev. Lett.* **54**, 1264 (1985).
- ⁶³J. Viñals and M. Grant, *Phys. Rev. B* **36**, 7036 (1987).
- ⁶⁴Y. Oono and S. Puri, *Phys. Rev. Lett.* **58**, 836 (1987).
- ⁶⁵R. Pindak, C. Y. Young, R. B. Meyer, and N. A. Clark, *Phys. Rev. Lett.* **45**, 1193 (1980).

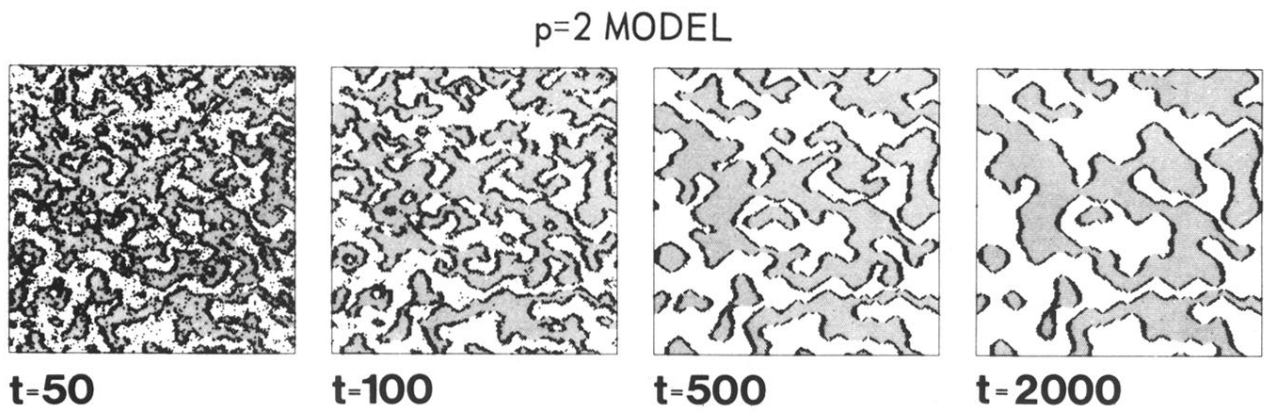


FIG. 2. Zero-temperature domain-wall network at different times t (in units of MCS/S) for the $p=2$ model with $P/J=2$ on a lattice with $N=200^2$ spins. The two ordered ground-state domains are indicated by white and grey regions separated by the black wall spins.

p=2 MODEL

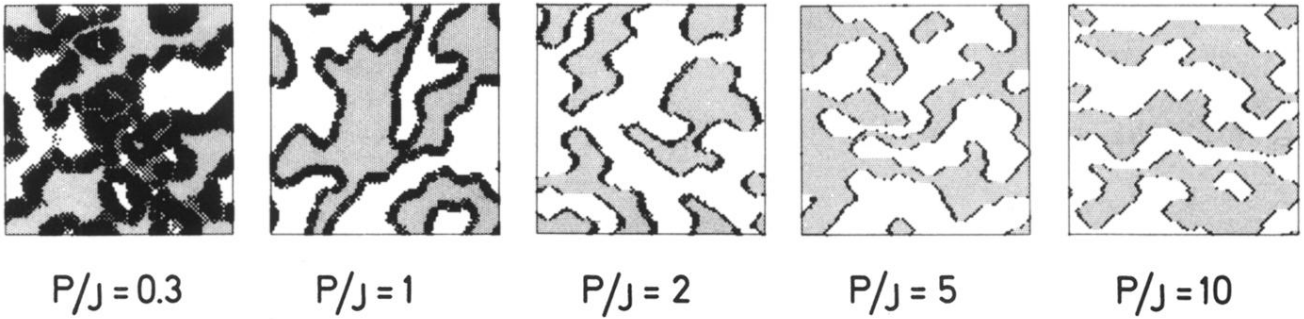


FIG. 3. Snapshots of zero-temperature domain-wall configurations for the $p=2$ model at $t=500$ MCS/S for different values of P/J . The model contains $N=100^2$ spins.